VILNIUS UNIVERSITY

FACULTY OF MATHEMATICS AND INFORMATICS

MATHEMATICS STUDY PROGRAMME

Master's Thesis

Analysis of the prime zeta function zeros placement patterns

Pirminių skaičių dzeta funkcijos nulių išsidėstymo tyrimas

YUNUS EMRE TUZCU

Supervisor : Prof. Dr. Igoris Belovas

Vilnius
2026

Acknowledgements

The author wishes to thank his supervisor, Prof. Dr. Igoris Belovas, for his constant support and valuable advice throughout the course of this research.

Summary

The prime zeta function, $P(s) = \sum_{p \in \mathbb{P}} p^{-s}$, encodes fundamental information about the distribution of prime numbers. Although its analytic continuation obtained via the Möbius inversion formula is well understood, the structure and placement patterns of its zeros remain underexplored. This thesis investigates the distribution of zeros of the prime zeta function in the complex plane, combining theoretical analysis with computational methods. The computational framework employs global optimization using the differential evolution algorithm to locate candidate zeros, which are subsequently verified by analyzing the intersections of the real and imaginary surfaces of the prime zeta function.

Analysis of 10318 zeros of the prime zeta function in the region $(\sigma, t) \in (0.1, 1.65) \times (0, 10^4)$ reveals several notable patterns. The distribution of real parts exhibits multimodality, with prominent peaks near $\sigma \approx 0.1$ and $\sigma \approx 0.6$. The zero counting function $N(T)$ exhibits $T \log T$-type growth, reminiscent of the Riemann-von Mangoldt formula for the Riemann zeta function. Furthermore, the spacing-ratio statistics show behavior similar to predictions from the Gaussian Unitary Ensemble (GUE). Together, these findings suggest that the high-lying zeros of the prime zeta function may asymptotically follow GUE-type statistics analogous to those conjectured for the zeros of the Riemann zeta function.

Keywords: prime zeta function, zeros distribution, analytic continuation, random matrix theory, spacing statistics, GUE conjecture

Santrauka

Pirminė dzeta funkcija, $P(s) = \sum_{p\in\mathbb{P}} p^{-s}$, apima esminę informaciją apie pirminių skaičių pasiskirstymą. Nors jos analizinis pratęsimas, išreikštas pasitelkiant Möbijaus apgręžimo formulę, yra gerai ištirtas, funkcijos nulių išsidėstymo stuktūra ir dėsningumai išlieka nepakankamai išnagrinėti. Šiame darbe tiriamas pirminės dzeta funkcijos nulių pasiskirstymas kompleksinėje plokštumoje, apjungiant teorinę analizę su skaitmeniniais metodais. Skaitiniai tyrimai remiasi globalia optimizacija, naudojančia diferencialinės evoliucijos algoritmą galimiems nuliams nustatyti. Vėliau kandidatai yra patikrinami analizuojant realiųjų ir menamųjų pirminės dzeta funkcijos paviršių susikirtimo kreivių elgesį.

Pirminių skaičių dzeta funkcijos 10 318 nulių analizė srityje $(\sigma,t) \in (0{,}1, 1{,}65) \times (0, 10^4)$ atskleidžia keletą pažymįtinų dėsningumų. Realiųjų dalių pasiskirstymas yra multimodalinis, su išreikštais pikais ties $\sigma \approx 0{,}1$ ir $\sigma \approx 0{,}6$. Nulių skaičiavimo funkcija $N(T)$ pasižymi $T \log T$ tipo augimu, primenančiu Riemanno–von Mangoldto formulę Riemanno dzeta funkcijai. Be to, tarpų santykių statistika elgiasi panašiai kaip prognozuojama Gauso unitarinio ansamblio (GUA) modelyje. Kartu šie rezultatai leidžia manyti, kad aukštai esantys pirminės dzeta funkcijos nuliai asimptotiškai gali paklusti GUE tipo statistikai, analogiškai tam, kas spėjama Riemanno dzeta funkcijos nuliams.

Raktiniai žodžiai: pirminių skaičių dzeta funkcija, nulių pasiskirstymas, analizinis pratęsimas, atsitiktinių matricų teorija, intervalų statistikos, GUA hipotezė.

List of Figures

List of Tables

Contents

List of symbols

- $\mathbb{R}$: the set of real numbers
- $\mathbb{N}$: the set of natural numbers
- $\mathbb{Z}$: the set of integers
- $\mathbb{P}$: the set of prime numbers
- $\mathbb{P}_n$: the set of first n prime numbers
- s: a complex variable, $s = \sigma + it$
- $P(s)$: the prime zeta function
- $\zeta(s)$: the Riemann zeta function
- $\mu(n)$: the Möbius function

List of abbreviations

GUE	Gaussian unitary ensemble
RSS	Residual sum of squares
KDE	Kernel density estimation
GMM	Gaussian mixture models
EMB	Empirical modified Borwein
BIC	Bayesian information criterion

1 Introduction

Zeta functions are important analytical tools, used to address underlying problems of the number theory, such as the distribution of prime numbers. Some of these functions, e.g., the Riemann zeta function, the Hurwitz zeta function, the Lerch zeta function, Dirichlet L-functions or zeta functions of the Selberg class, have been extensively studied, while others have received minimal attention. A perfect example of such a function is the prime zeta, one of the most under-researched varieties of the class (see [2, 6]).

1.1 Prime zeta function

In contrast to the Riemann zeta function, the analytic properties of the prime zeta function are more intricate due to its dependence on the zeros of the Riemann zeta function. In particular, the location of singularities and the possibility of analytic continuation are closely related to the distribution of nontrivial zeros of the Riemann zeta function. Understanding the behavior of prime zeta function, especially the placement of its zeros and singularities, provides additional insight into prime number theory and complements classical results related to the Riemann zeta function. Let $s = \sigma + it$ be a complex variable and $\mathbb{P}$ be the set of prime numbers. For $\sigma > 1$, we define the prime zeta function by the following expression,

$$P(s) = \sum_{p \in \mathbb{P}} \frac{1}{p^s}. \tag{1}$$

In the half-plane $\sigma > 1$, the series converges absolutely. The next important formula was given by Glaisher [7],

$$P(s) = \sum_{n=1}^{\infty} \frac{\mu(n)}{n} \log \zeta(ns). \tag{2}$$

Formula (2) provides an analytic continuation of the prime zeta function to the critical strip $0 < \sigma \leq 1$. Landau and Walfisz showed that the prime zeta function cannot be continued to the half-plane $\sigma \leq 0$ [8]. This is due to the clustering of singular points along the imaginary axis arising from the nontrivial zeros of the Riemann zeta function on the critical line. This representation also identifies the singularities of $P(s)$: they occur at points $s = 1/k$ and $s = \rho/k$, where k is square-free and ρ is a zero of the Riemann zeta function $\zeta(s)$. For calculations of $\log(\zeta(ns))$ throughout all calculations, we use the principal branch of logarithm.

1.2 Problem statement

The thesis investigates the distribution of zeros of the prime zeta function $P(s)$ in the complex plane. Although the analytic continuation of $P(s)$ is well understood, the structure and distribution of its zeros remain less explored. In particular, this work aims to analyze how the zeros of $P(s)$ are influenced by the zeros of the Riemann zeta function $\zeta(s)$, and whether identifiable patterns or regularities emerge.

1.2.1 Definition. A point $s_0 \in \mathbb{C}$ is called a candidate zero of the prime zeta function if

$$|P(s_0)| < \varepsilon,$$

for a prescribed tolerance $\varepsilon > 0$.

We aim to identify candidate zeros and subsequently verify their validity.

1.3 Rationale and significance of the research

The study of the prime zeta function is closely connected to fundamental questions in number theory, especially those concerning the distribution of prime numbers. Since $P(s)$ is directly defined in terms of primes, understanding its analytic structure contributes to a deeper understanding of prime-related phenomena. Moreover, the connection between $P(s)$ and $\zeta(s)$ via identities such as (2) implies that the behavior of $P(s)$ reflects properties of the Riemann zeta function, including its zeros. Therefore, investigating the zeros of $P(s)$ may provide complementary perspectives on classical conjectures and results in analytic number theory. From a practical standpoint, advances in computational methods allow for numerical exploration of these functions, making it possible to detect patterns that may not be accessible through purely theoretical means.

1.4 Object of the research

The object of this research is the prime zeta function $P(s)$ as a complex-valued function defined on subsets of the complex plane. The study focuses on the distribution of its zeros.

1.5 Aim and objectives of the research

The main aim of this thesis is to analyze the placement patterns of zeros of the prime zeta function and to understand their underlying structure. To achieve this aim, the following objectives are formulated:

- To review the analytic properties of the prime zeta function and its relation to the Riemann zeta function.
- To examine theoretical criteria governing the presence or exclusion of zeros in certain regions of the complex plane.
- To analyze numerical methods for locating and validating zeros of the prime zeta function and identify possible patterns in their distribution.

1.6 Methodological overview

This research combines analytical and computational methods. The analytical part relies on classical results from analytic number theory. The computational part involves numerical evaluation of the prime zeta function using various algorithms employing the Riemann zeta function subroutines. For efficient computation of Riemann zeta function, we use EMB-algorithm [3]. Parallel computation was implemented using the `workers` parameter of `scipy.optimize.differential_evolution`. The `differential_evolution` routine is a stochastic global optimization algorithm based on the Differential Evolution method, where candidate solutions evolve iteratively through mutation, recombination, and selection operations.

Visualization and data analysis techniques are used to interpret the numerical results and to detect potential patterns in the zero distribution.

All numerical experiments, optimization procedures, and visualization scripts used in this thesis were implemented in Python. The complete source code is publicly available [12].

1.7 Scientific novelty and practical value of the work

The scientific novelty of this work lies in the systematic investigation of the zero distribution of the prime zeta function, a topic that has received relatively limited attention compared to other zeta functions.

The thesis introduces a reproducible computational framework that combines differential evolution global optimization, contour-based zero verification and statistical modeling techniques for the study of prime zeta zeros. In particular, the work extends previous numerical investigations by independently recomputing and validating zeros of the prime zeta function using additional numerical consistency checks.

The main original contributions of the thesis are the following:

- A large-scale numerical analysis of 10318 zeros of the prime zeta function in the region

  $$(\sigma,t) \in (0.1, 1.65) \times (0, 10^4),$$

  including independent validation of the detected zeros through contour-based methods.

- Providing numerical evidence that the real parts of the zeros exhibit a stable multimodal distribution rather than concentrating near a single vertical line.

- Numerical evidence that the zero-counting function of the prime zeta function follows an asymptotic law of the form

  $$N(T) \sim aT \log T,$$

  analogous to the Riemann–von Mangoldt formula for the Riemann zeta function, but with a different leading constant.

- Investigation of local spacing-ratio statistics for zeros of the prime zeta function, together with numerical evidence that the high-lying zeros exhibit behavior compatible with Gaussian Unitary Ensemble (GUE) statistics from random matrix theory.
- The formulation of new conjectures concerning the asymptotic distribution, counting function growth, and spacing statistics of prime zeta zeros based on the observed numerical data.

The practical value of the work lies in the development of computational tools and numerical methodologies that can be reused for further investigations of the prime zeta function.

1.8 Structure of the thesis

The thesis is organized as follows. The introduction presents the problem, the aim and the objectives, novelty and significance of the research. The analytical part reviews the theoretical background, including known results about the prime zeta function, and introduces the methods used in the study. The experimental part describes the computational approach, presents the data and results, and provides an analysis of the observed patterns. Finally, the conclusions summarize the main findings. The last two sections present conclusions and possible directions for future research.

2 Analytical part

Despite its apparently elementary definition (cf. (1)), the analytic structure of the prime zeta function $P(s)$ is remarkably intricate and is closely connected to properties of the zeros of the Riemann zeta function.

2.1 Literature survey

The systematic study of the prime zeta function begins with the classical identity

$$\log \zeta(s) = \sum_{n=1}^{\infty} \frac{P(ns)}{n},$$

which follows from Euler's product formula by logarithmic expansion. Applying Möbius inversion [11] yields the fundamental representation

$$P(s) = \sum_{n=1}^{\infty} \frac{\mu(n)}{n} \log \zeta(ns),$$

where $\mu(n)$ stands for the Möbius function (Glaisher [7]). This representation is valid initially for $\mathsf{Re}(s) > 1$ and subsequently extended into the half-plane $\mathsf{Re}(s) > 0$. This identity plays a central role throughout the literature, since it transfers analytic information about $\zeta(s)$ directly to $P(s)$.

A decisive contribution to the theory was made by Landau and Walfisz [8], who investigated the analytic continuation properties of the function

$$Q(s) = \sum_{p} \frac{\log p}{p^s} = -P'(s).$$

Using the analytic continuation of $\zeta(s)$ together with zero-density information for its nontrivial zeros, Landau and Walfisz established that $Q(s)$ admits a meromorphic continuation to the half-plane $\mathsf{Re}(s) > 0$, where all singularities are simple poles. More importantly, they proved that neither $Q(s)$ nor $P(s)$ can be analytically continued beyond the line $\mathsf{Re}(s) = 0$.

A substantially more detailed analytic and computational investigation was later carried out by Fröberg [6]. Whereas Landau and Walfisz [8] concentrated primarily on analytic continuation and natural boundaries, Fröberg examined the global analytic behavior of $P(s)$, including its singularities, zeros and numerical values. He emphasized the role of the representation (2) as the principal tool for numerical computation and analytic continuation. From this formula, he observed that singularities occur not only through the nontrivial zeros of $\zeta(s)$, but also at points $s = 1/k$, where k is square-free, arising from the pole of $\zeta(s)$ at $s = 1$. Consequently, the singular structure of $P(s)$ consists simultaneously of isolated real singularities and infinitely many complex logarithmic singularities generated by the zeros of $\zeta(s)$.

Fröberg further investigated the local behavior near $s = 1$, deriving the asymptotic expansion

$$P(1+\varepsilon) = \log\frac{1}{\varepsilon} + C + O(\varepsilon), \tag{3}$$

where $\varepsilon > 0$ and

$$C = \sum_{n=2}^{\infty} \frac{\mu(n)}{n} \log\zeta(n).$$

The modern study of the prime zeta function has increasingly shifted toward questions concerning its statistical behavior, computation and the geometric distribution of its zeros, and its relation to the structure of the zeros of the Riemann zeta function.

A significant probabilistic approach to the prime zeta function was developed by Chavez and Allawala [4]. Using Lyapunov's central limit theorem and Mertens' second theorem, the paper shows that as $t \to \infty$:

$$\frac{1}{\sqrt{\frac{1}{2}\log\log t}} \operatorname{Re} P_t(1/2 + i\tau) \xrightarrow{d} \mathcal{N}(0,1),$$

and similarly for the imaginary part

$$\frac{1}{\sqrt{\frac{1}{2}\log\log t}} \operatorname{Im} P_t(1/2 + i\tau) \xrightarrow{d} \mathcal{N}(0,1).$$

The variance is:

$$\operatorname{var}\{\operatorname{Re} P_t(1/2 + i\tau)\} = \frac{1}{2}\log\log t + O(1),$$

where

$$P_t(s) = \sum_{p \le t} \frac{1}{p^s}.$$

A different line of investigation was pursued by Belovas et al. [2] which focuses on the computation and distribution of zeros of the prime zeta function. The following theorem about a zero-free region was proved.

2.1.1 Theorem. *The prime zeta function has no zeros in the half-plane $\sigma > \sigma_0$. Here $\sigma_0 =$ $1.77954465354699\ldots$ is the zero of the function $U(\sigma) = 2^{1-\sigma} - P(\sigma)$.*

Note that the result of Theorem 2.1.1 can not be refined by more than $\Delta = 0.097$, since if $M = 200000$ and

$$\sigma_T = \max_{|t|<T}\{\ \sigma \mid P(\sigma) = 0\ \}, \tag{4}$$

then the authors obtained

$$\sigma_M = 1.682628788045196....$$

Thus the smallest σ' such that $P(s)$ has no zeros for $\sigma > \sigma'$ satisfies $\sigma_M < \sigma' < \sigma_0$. Next, the authors identified a total of 10318 candidate zeros in the rectangle $(0.1; \sigma_0) \times (0; 10^4)$. They proposed and tested the following three conjectures concerning the underlying layout patterns of the prime zeta function zeroes.

2.1.2 conjecture. *The estimate for the zero-free plane given by Theorem 2.1.1 can not be improved, that is*

$$\lim_{T\to\infty} \sigma_T = \sigma_0. \tag{5}$$

2.1.3 conjecture. *Let* $0 < \gamma < \sigma_0$ *and*

$$L_\gamma(x,T) = \#\{s \mid P(s) = 0,\ \sigma > \gamma,\ 0 < t/T < x\},$$

then the imaginary parts of the zeros of the prime zeta function $\operatorname{Im} s$ *are distributed uniformly, i.e., for* $\gamma \geqslant 1$ *and* $0 < x < 1$*, we have*

$$\lim_{T\to\infty} \frac{L_\gamma(x,T)}{L_\gamma(1,T)} \Rightarrow \mathbb{U}(0,1). \tag{6}$$

2.1.4 conjecture. *Let* $0 < \gamma < \sigma_0$ *and*

$$M_\gamma(T) = \#\{s \mid P(s) = 0,\ \sigma > \gamma, 0 < t < T\},$$

then there are positive constants c *and* C *(maybe depending on* γ*), such that the inequality*

$$cT < M_\gamma(T) < CT \tag{7}$$

holds, for $\gamma > 1$ *and* T *large enough. The weaker proposition is* $M_1(T) = O(T)$*.*

3 Experimental part

3.1 Computation of zeros of the prime zeta function

The series (1) converges very slowly. For example, for $s = 2$, to get 7 decimals of accuracy, we need around 56000 terms (exactly 56161), i.e.,

$$\left| P(s) - \sum_{p \in \mathbb{P}_{56161}} \frac{1}{p^s} \right| < 10^{-7} < \left| P(s) - \sum_{p \in \mathbb{P}_{56160}} \frac{1}{p^s} \right|$$

where $\mathbb{P}_n$ denotes set of first n primes. Note that it converges even slower as σ and t get smaller. Since we know the zeros are in the region $\sigma < 2$, this is not a good calculation method. Figure 1 illustrates this series's performance.

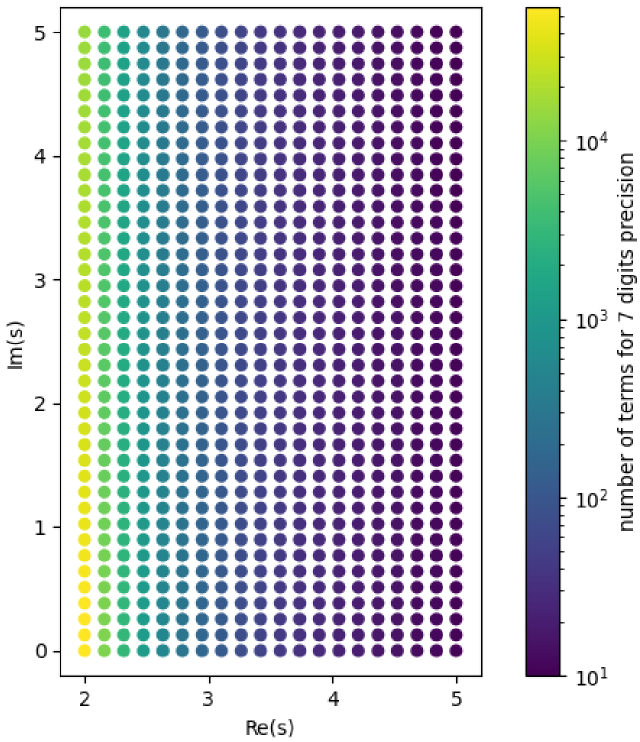

1 Figure *Number of terms needed to calculate s to 7 decimals (colors are logarithmic scale)*

- `Algorithm 1`: Note that $\log \zeta(ns) = O(2^{-n\sigma})$. Hence, the series (2) converges rapidly enough to allow precise calculations. This algorithm relies on Möbius function and the Riemann zeta function. The Möbius function is defined as follows

$$\mu(n) = \begin{cases} 1 & \text{if } n = 1, \\ 0 & \text{if } n \text{ contains a square factor,} \\ (-1)^q & \text{if } n \text{ is the product of } q \text{ different prime factors} \end{cases}$$

For the calculation of Riemann zeta function in `Algorithm 1` and `Algorithm 2`, we use python's `mpmath.zeta`. Compared to series (1), this algorithm runs much faster. See image below for comparison.

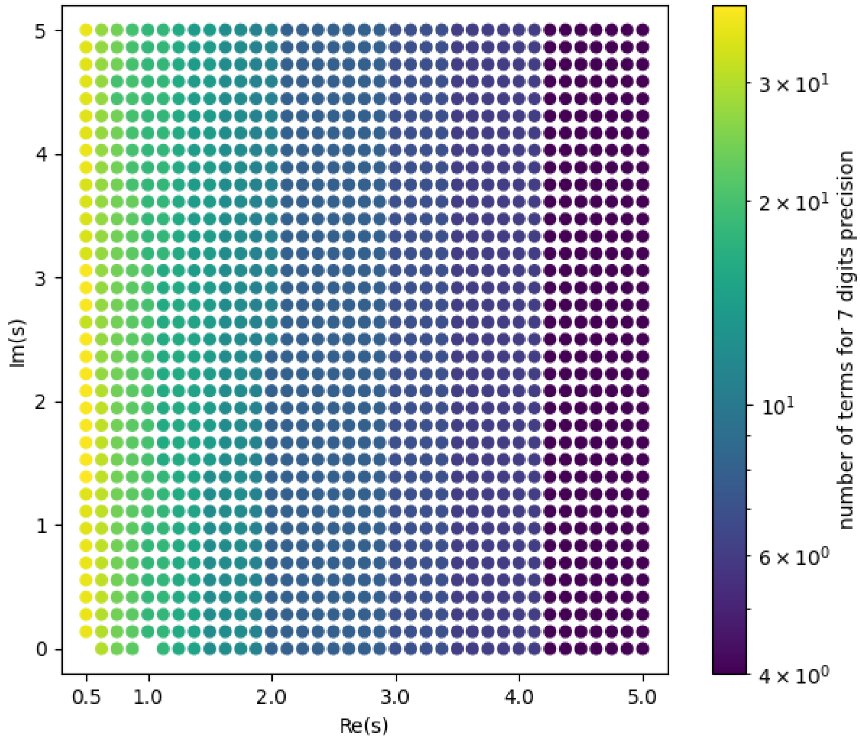

2 ***Figure*** *Number of terms needed to calculate s to 7 decimals*

Notice that the color chart goes up to 39 compared to 56161 in Figure 1. In addition, we could extend the region to $\sigma \geq 0.5$ without significant calculation time change. Also, notice we are missing value for points $s = 0.5$ and $s = 1$. This is due to the singularities of prime zeta function.

- `Algorithm 2`: Hybrid partial-sum method

  Following Cohen [5] and Belovas [2], the convergence can be improved further by separating the contribution of small primes.

  Define

$$\zeta_{p>A}(s) = \zeta(s) \prod_{p \leq A} \left(1 - \frac{1}{p^s}\right)$$

  where $A \in \mathbb{N}$ is a cutoff parameter. Then

$$P(s) = \sum_{p \leq A} \frac{1}{p^s} + \sum_{n=1}^{\infty} \frac{\mu(n)}{n} \log \zeta_{p>A}(ns)$$

Since

$$\log \zeta_{p>A}(ns) = O(A^{-n\sigma}),$$

the convergence rate improves substantially for moderate values of A. In practice, the parameter A was selected empirically to balance the cost of the finite prime summation and the speed of convergence of the remainder term. This method achieved the best overall performance for large-scale searches.

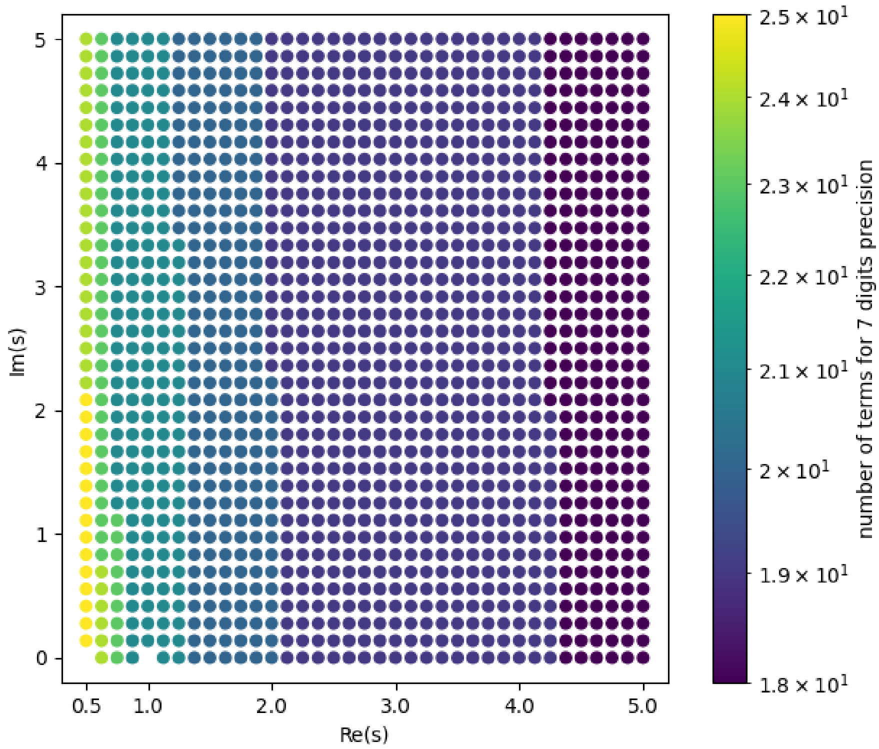

3 ***Figure*** *Number of terms needed to calculate s to 7 decimals*

The maximum number of required terms decreases further from 39 to approximately 25.

- `Algorithm 3`: EMB-enhanced computation

  The final implementation used the EMB-algorithm proposed in [3] to accelerate the computation of the Riemann zeta function appearing in `Algorithm 2`. This optimization reduced the total evaluation time of $P(s)$ and enabled large-scale searches over extensive regions of the complex plane.

3.2 Localization of candidate zeros of the prime zeta function

The numerical search for zeros of the prime zeta function was performed by combining global optimization methods with contour-based verification. The complex plane was partitioned into rectangular regions of size $[\sigma_1, \sigma_2] \times [t, t+1]$. Each rectangle was processed independently. To detect zeros, the following real-valued objective function was introduced:

$$f(\sigma,t) = |P(s)|^2. \tag{8}$$

Since

$$f(\sigma,t) = 0 \iff P(s) = 0,$$

finding zeros of $P(s)$ is equivalent to minimizing $f(\sigma,t)$.

For each rectangle, a global optimization procedure based on the differential evolution algorithm

`scipy.optimize.differential_evolution`

was applied. Differential evolution is particularly suitable in this setting because:

- the objective function is highly oscillatory,
- local minima occur frequently,
- derivatives are not required,
- the method is less sensitive to the initial guess than local optimization algorithms.

To assess the robustness of the optimization procedure, the differential evolution algorithm was repeated using several random seeds and optimization tolerances. The resulting minimizers were found to agree to high numerical precision across all runs, indicating that the detected zeros are stable with respect to stochastic initialization and parameter selection. In addition, the objective values remained consistently close to zero, suggesting that the detected minima are not artifacts of the optimization procedure.

The search region for each optimization step was defined by

$$\sigma \in [\sigma_1,\sigma_2], \qquad t \in [t,t+1].$$

The optimization algorithm minimized the objective function (8) over the rectangle.

The implementation used parallel processing to evaluate the objective function simultaneously on multiple CPU cores. The numerical experiments in this thesis were performed using 11 worker processes. The following simplified pseudocode summarizes the procedure:

1. Partition the strip into rectangles of height 1.
2. For each rectangle:
   (a) Minimize $f(\sigma,t)$ using differential evolution.
   (b) Record the minimizer (σ^*,t^*) and the corresponding value of the objective function f^*.
   (c) If f^* is below a prescribed tolerance, mark the point as a candidate zero.

The optimization process produces candidate points (σ^*, t^*), for which $f(\sigma^*, t^*) < \varepsilon$, where ε is a small numerical threshold.

However, small values of f^* alone are insufficient to rigorously confirm the existence of a zero, since numerical optimization may converge to near-minima or flat regions. Therefore, an additional validation step was performed.

3.3 Validation of candidate zeros of the prime zeta function

Candidate zeros were validated using contour plots of the real and imaginary parts of the prime zeta function in a neighborhood of each minimizer

$$s^* = \sigma^* + it^*.$$

After computing $P(s)$ using `Algorithm 3`, the function was evaluated on a fine rectangular grid

$$s_{jk} = \sigma_j + it_k.$$

The zero level sets

$$\mathsf{Re}(P(s)) = 0 \qquad \text{and} \qquad \mathsf{Im}(P(s)) = 0$$

were then generated using the routine

`matplotlib.pyplot.contour`.

A point was accepted as a genuine zero only when the two contours intersected transversally near the candidate point. This provides a consistency check that both the real and imaginary parts vanish simultaneously and helps distinguish genuine zeros from numerical artifacts. Figure 4 illustrates a typical verification plot.

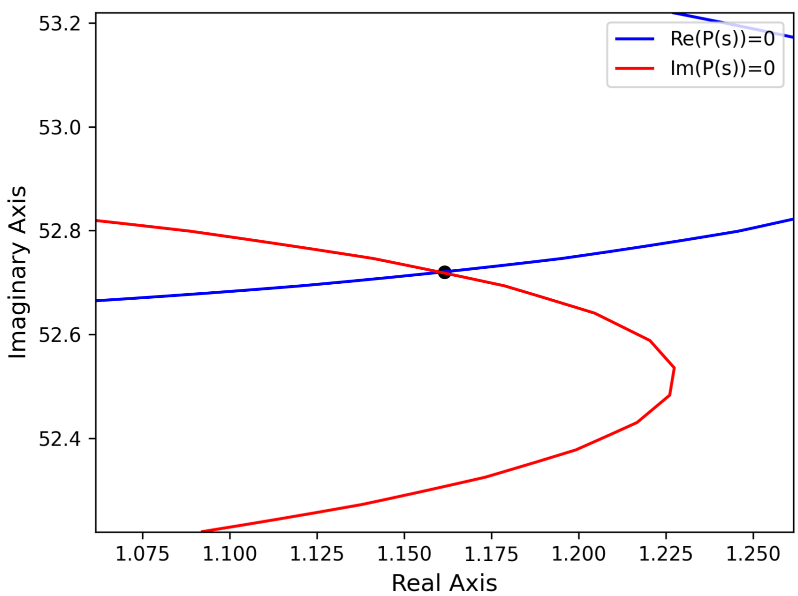

4 ***Figure*** *Contour-based validation of a candidate zero.*

Due to the high computational cost of contour verification for zeros with small real parts, a complete validation was not performed for every zero reported by Belovas et al. [2]. Instead, contour verification was carried out for a randomly selected 20% sample of the zeros in the computationally demanding region $0.1 < \sigma < 0.3$, while all remaining zeros on $\sigma \geq 0.3$ region were fully checked. No false positives were identified during this verification process.

Finally, selected zeros were recomputed with increased numerical precision and smaller optimization tolerances. The resulting approximations remained stable across repeated computations, indicating numerical reliability of the detected zeros.

3.4 Results and analysis

To locate zeros of the prime zeta function, we performed search in the region $0.3 \leq \sigma \leq 1.78, 0 \leq t \leq 6000$. In total, 4571 zeros were detected, as shown in Figure 5a. All zeros detected in the present investigation were independently validated using the contour-based procedure described in Section 3.3.

Given the time and calculation complexities, we have not extended the zero search region. For the analysis of the distribution of zeros, we used the zeros found in rectangle $0.1 < \sigma < 1.65$, $0 < t < 10^4$ by Belovas et al. [2], shown in Figure 5b.

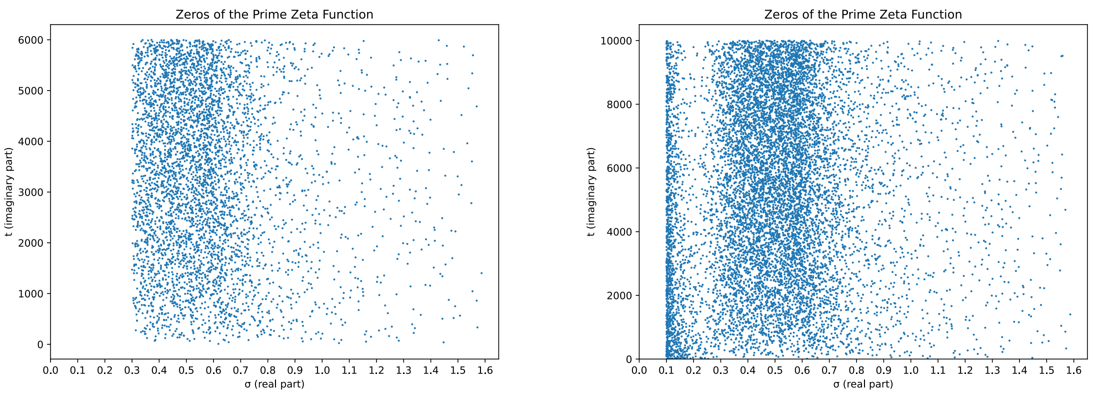

(a) Zeros found from our research *(b) 10318 zeros found by Belovas et al. [2]*

5 Figure *Combined plots of zeros*

3.4.1 Distribution of the real parts of zeros of the prime zeta function

To investigate the distribution of the real parts of the zeros, we study the empirical distribution using histograms and Gaussian kernel density estimation.

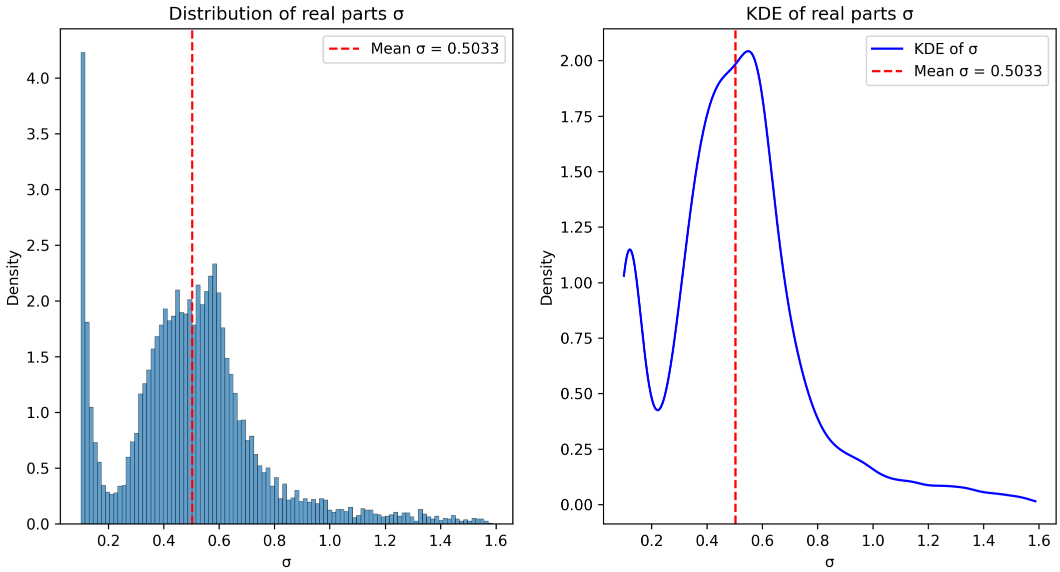

6 Figure *Standard histogram vs Gaussian KDE*

Figure 6 displays both the empirical histogram and the Gaussian kernel density estimator (KDE) of the real parts. The empirical distribution is visibly non-Gaussian and exhibits two dominant concentrations near

$$\sigma \approx 0.1, \qquad \sigma \approx 0.6.$$

To quantify these features, we computed the sample skewness, kurtosis, and Hartigan's dip statistic for multimodality. The dip test rejects the null hypothesis of unimodality at significance level 10^{-6}, providing strong statistical evidence that the distribution is not generated by a single unimodal population.

To further investigate the apparent multimodal structure, Gaussian mixture models (GMMs) with varying numbers of components were fitted to the data, and model selection was performed using the Bayesian Information Criterion (BIC). The BIC values favor a four-component model, which substantially outperforms the corresponding two- and three-component fits. The estimated component means are

$$\{0.974, 0.594, 0.409, 0.119\},$$

with corresponding mixture weights

$$\{0.110, 0.358, 0.414, 0.117\}.$$

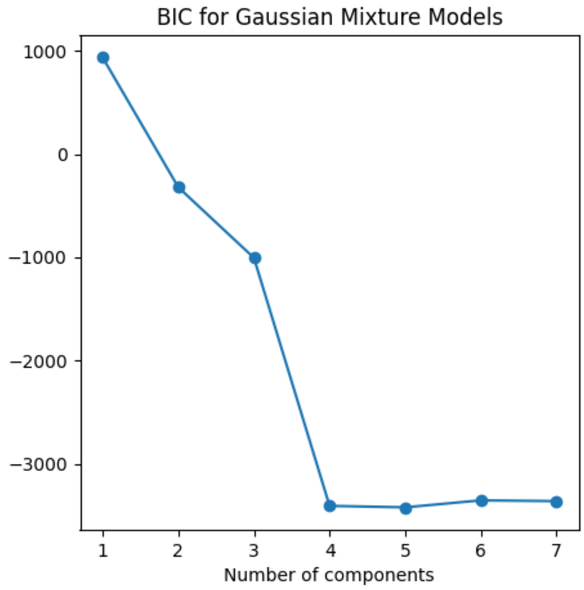

7 ***Figure*** *BIC for Gaussian Mixture Models*

Models with $k \geq 5$ components yield only marginal improvements in BIC while introducing components with very small weights, indicating possible overfitting. Figure 7 illustrates the BIC comparison across different model sizes.

3.4.1 conjecture. *The empirical distribution of the real parts of the zeros of $P(s)$ does not concentrate to a single limiting value. Instead, several persistent concentration regions appear at large heights.*

To assess the stability of the observed multimodal structure, a bootstrap analysis of the Gaussian mixture model was performed. Using 100 bootstrap resamples, the four-component Gaussian mixture model was repeatedly refitted to randomly resampled datasets. The estimated component means μ_n, ordered increasingly for $n = 1,2,3,4$, were found to be

$$\mu_1 = 0.1195 \pm 0.0013, \qquad \mu_2 = 0.4117 \pm 0.0048,$$

$$\mu_3 = 0.5968 \pm 0.0039, \qquad \mu_4 = 0.9808 \pm 0.0166,$$

where the uncertainties denote the standard deviations across bootstrap samples.

The relatively small fluctuations in the estimated component locations indicate that the observed clusters are stable under resampling and are therefore unlikely to arise solely from statistical noise or kernel smoothing artifacts.

The bootstrap fluctuations are smallest for the component near $\sigma \approx 0.12$, indicating that this concentration is particularly stable under resampling. The components near $\sigma \approx 0.41$ and $\sigma \approx 0.60$ also exhibit relatively small variability, suggesting that these features are robust characteristics of the empirical distribution.

In contrast, the component near $\sigma \approx 0.98$ displays noticeably larger uncertainty. This may reflect a smaller effective sample size, weaker separation from neighboring regions, or boundary effects near $\sigma = 1$. Consequently, while the numerical analysis provides evidence for several persistent concentrations in the distribution of real parts, the precise number and interpretation of these components should be treated cautiously.

In particular, the persistence of several well-separated components provides additional numerical support for Conjecture 3.4.1.

3.4.2 Counting function

For a sequence of imaginary parts of zeros $\{t_n\}$ ordered increasingly, the counting function $N(T) = \#\{n : t_n \leq T\}$ encodes the average density. For the Riemann zeta function, the Riemann-von Mangoldt formula states

$$N_\zeta(T) = \frac{T}{2\pi} \log \frac{T}{2\pi e} - \frac{T}{2\pi} + O(\log T).$$

We formulate a conjecture that states similar asymptotic behaviour for the prime zeta function's counting function.

3.4.2 conjecture. *Let $N(T) = \#\{s = \sigma + it : P(s) = 0,\ 0 < t \leq T\}$ be the counting function for zeros of the prime zeta function in the upper half-plane. Then there exists a constant $a > 0$ such that, as $t \to \infty$,*

$$N(T) \sim aT \log T.$$

In search for similar asymptotic behaviour, we fit the following model to our data:

$$N(T) \sim aT \log T + bT + c.$$

The fitted parameters were estimated together with their standard uncertainties obtained from the covariance matrix of the nonlinear least-squares fit:

$$a = 0.100955 \pm 0.000056 \qquad b = 0.101883 \pm 0.000527 \qquad c = 0.721796 \pm 0.226899$$

The relatively small uncertainties indicate that the logarithmic model is stable over the investigated range. To examine the leading asymptotic behavior directly, the ratio

$$\frac{N(T)}{T \log T}$$

was computed numerically.

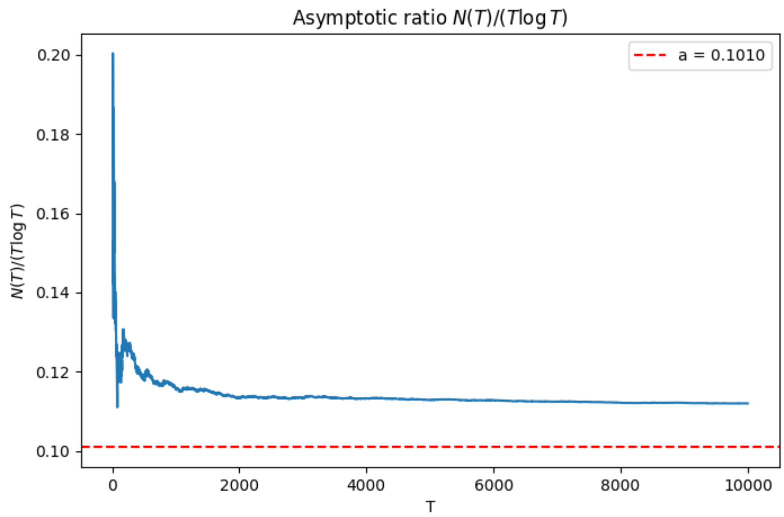

8 Figure *Asymptotic behaviour of the ratio*

The ratio appears to vary slowly for large T, remaining within a relatively narrow range and exhibiting only mild downward drift, as shown in Figure 8. This behavior is consistent with the hypothesis that the leading-order growth of the counting function is proportional to $T \log T$, although the presently accessible range is insufficient to determine the limiting constant reliably.

To test the consistency of this asymptotic form, the quantity

$$R_a(T) = \frac{N(T) - bT - c}{T \log T}$$

was analyzed numerically.

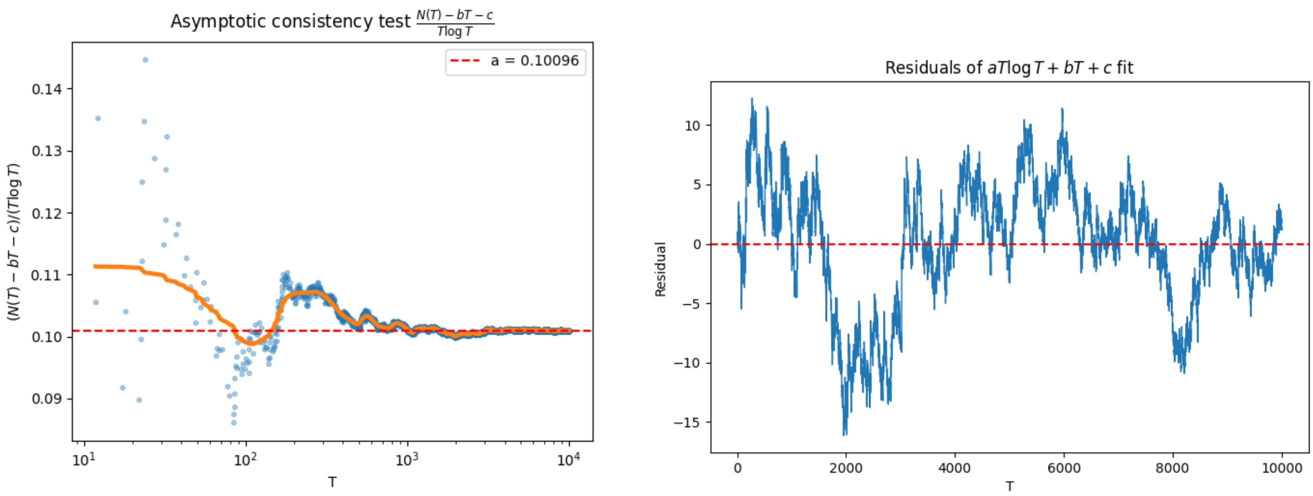

(a) *Asymptotic consistency test*

(b) *Residuals of the model*

After the initial finite-size fluctuations, the ratio remained relatively stable in the high-T regime, taking values close to 0.101, as shown in Figure 9a. This suggests that substantial lower-order corrections are still present at the investigated heights. Nevertheless, the observed behavior remains compatible with convergence toward the fitted coefficient $a = 0.10096$ at larger values of T.

To assess the quality of the asymptotic approximation further, the residuals

$$N(T) - (aT \log T + bT + c)$$

were analyzed.

The residual plot shown in Figure 9b does not exhibit significant systematic drift over the investigated range, indicating that the logarithmic model captures the dominant growth behavior of the counting function. The remaining fluctuations are consistent with finite-size effects and lower-order corrections. Consequently, the numerical data support Conjecture 3.4.2, while also indicating that finite-size effects and lower-order corrections remain significant over the investigated range.

While the presently accessible range of T is insufficient for a rigorous asymptotic determination, the evidence strongly indicates that the zeros of the prime zeta function obey a logarithmic counting law qualitatively similar to that of the Riemann zeta zeros, but with a distinctly different normalization constant.

3.4.3 Spacing ratio statistics

For a sequence of imaginary parts of zeros $\{t_n\}$ ordered increasingly, define $s_n = t_{n+1} - t_n$. The ratio of consecutive spacings,

$$r_n = \frac{\min(s_n, s_{n+1})}{\max(s_n, s_{n+1})}, \quad r_n \in [0, 1], \tag{9}$$

introduced by Oganesyan and Huse [10], provides a local spectral statistic that does not require unfolding. Closed-form random matrix predictions for the corresponding ratio distributions were later derived in [1]. The theoretical distributions are:

$$P_{\text{Poisson}}(r) = \frac{2}{(1+r)^2}, \qquad \langle r \rangle_P = 2 \ln 2 - 1 \approx 0.3863, \tag{10}$$

$$P_{\text{GUE}}(r) = \frac{81\sqrt{3}}{4\pi} \frac{(r + r^2)^2}{(1 + r + r^2)^4}, \qquad \langle r \rangle_{\mathsf{GUE}} \approx 0.6027. \tag{11}$$

3.4.3 Remark. The distribution $P_{\mathsf{GUE}}(r)$ is normalized according to the convention used in [1],

$$\int_0^1 P_{\mathsf{GUE}}(r)\, dr = \frac{1}{2},$$

so that the corresponding probability density on [0,1] is given by $2P_{\mathsf{GUE}}(r)$. Consequently,

$$\langle r \rangle_{\mathsf{GUE}} = 2 \int_0^1 r\, P_{\mathsf{GUE}}(r)\, dr = \frac{2\sqrt{3}}{\pi} - \frac{1}{2} \approx 0.6027.$$

Next we formulate a conjecture concerning the spacing ratio statistics for the imaginary parts of the prime zeta function zeros.

3.4.4 conjecture. *The local spacing statistics of the high-lying zeros of the prime zeta function asymptotically follow the predictions of the Gaussian Unitary Ensemble (GUE). In particular, for the consecutive spacing ratios* r_n*,*

$$\lim_{N\to\infty} \frac{1}{N}\#\{n \le N : r_n \le r\} = 2\int_0^r P_{GUE}(x)\,dx,$$

where $P_{GUE}(r)$ *is given in* (11)*.*

For the full data set, the mean spacing ratio was found to be **0.5544**, which is substantially above the Poisson value **0.3863** and below the GUE value **0.6027**.

1 Table *Effect of increasing threshold for imaginary part*

Threshold Condition	Mean Spacing Ratio $\langle r\rangle$	Variance $\mathsf{Var}(r)$	Number of zeros
$t \ge 0$	0.5544	0.0824	10316
$t \ge 1000$	0.5654	0.0807	9516
$t \ge 2000$	0.5726	0.0794	8591
$t \ge 3000$	0.5799	0.0786	7593
$t \ge 4000$	0.5855	0.0772	6557
$t \ge 5000$	0.5882	0.0769	5509
$t \ge 6000$	0.5920	0.0755	4427
$t \ge 7000$	0.5932	0.0757	3346
$t \ge 8000$	0.5913	0.0753	2249
$t \ge 9000$	0.5989	0.0752	1123

Table 1 shows the behavior of the mean spacing ratio and variance after progressively excluding low-lying zeros. The numerical results indicate a gradual increase in the mean consecutive spacing ratio as the height threshold increases. In particular, the values approach the GUE prediction

$$\langle r\rangle_{\mathsf{GUE}} \approx 0.6027.$$

To further investigate Conjecture 3.4.4 and assess the stability of the observed spacing ratio behavior, a nonparametric bootstrap procedure with 5000 resamples was used to estimate a 95% confidence interval for the mean spacing ratio. The resulting interval was

$$0.5828 \le \langle r\rangle \le 0.6155,$$

with the GUE prediction lying well within the confidence interval.

These observations support the conjecture that the high-lying zeros asymptotically exhibit GUE-type local statistics analogous to those conjectured for the nontrivial zeros of the Riemann zeta function (see [9]). However, the dataset remains relatively small compared to large-scale studies of Riemann zeta zeros, and therefore the observed agreement with GUE statistics should be interpreted cautiously.

4 Conclusions

This thesis investigated the distribution and statistical properties of the zeros of the prime zeta function $P(s)$ through a combination of analytic methods and large-scale numerical computations. The main findings are summarized as follows:

1. **Numerical framework for zero detection.**

   A computational framework for locating and validating zeros of $P(s)$ was developed using global optimization methods combined with contour-based verification. In addition to detecting 4571 zeros in the investigated region, the method was used to partially validate the 10318 zeros previously reported by Belovas et al. [2]. No false positives were identified, providing strong numerical evidence for the reliability and reproducibility of the previously obtained zero dataset. The resulting framework enabled large-scale statistical analysis of the zero distribution.

2. **Multimodal distribution of real parts of zeros.** The histogram of real parts of zeros exhibits two distinct peaks: a sharp peak near $\sigma \approx 0.1$ and a broader peak centered at $\sigma \approx 0.6$. Gaussian mixture modeling and bootstrap analysis demonstrated that these concentration regions remain stable under resampling, providing evidence that the observed structure is intrinsic rather than a numerical artifact. These observations suggest that the zeros of the prime zeta function may organize into several persistent vertical concentration bands rather than accumulating near a single preferred real part. This behavior is conjectured in Conjecture 3.4.1.

3. **Counting function asymptotics.** The zero-counting function

   $$N(T) = \#\{s = \sigma + it : P(s) = 0,\ 0 < t \leq T\}$$

   was numerically investigated and found to be well approximated by the asymptotic model

   $$N(T) \sim aT \log T + bT + c.$$

   The fitted coefficient $a \approx 0.101$ remained stable across the investigated range, while residual analysis showed no substantial systematic drift. The numerical results therefore support the conjecture that the dominant growth of the counting function is proportional to $T \log T$, analogous to the Riemann–von Mangoldt law for the zeros of $\zeta(s)$, although with a different normalization constant.

4. **Spacing statistics and GUE conjecture.** The local spacing statistics of the imaginary parts of the zeros were analyzed using consecutive spacing ratios. The empirical mean ratio was observed to increase toward the Gaussian Unitary Ensemble (GUE) prediction as low-lying zeros were excluded from the dataset. Bootstrap confidence intervals further

supported consistency with GUE-type statistics. These findings provide numerical evidence that the high-lying zeros of the prime zeta function may exhibit statistical behavior similar to that conjectured for the nontrivial zeros of the Riemann zeta function. The observed convergence toward the GUE prediction suggests that the local spacing structure becomes increasingly regular at higher heights.

Overall, the results of this thesis demonstrate that the prime zeta function possesses a surprisingly rich and highly structured zero distribution. Although many of the observed phenomena remain conjectural, the numerical evidence indicates that the zeros of $P(s)$ exhibit nontrivial geometric and statistical regularities closely connected to the analytic behavior of the Riemann zeta function. The developed computational framework and the statistical observations obtained in this work provide a foundation for future theoretical and numerical investigations of the prime zeta function.

5 Future research directions

Several avenues for extending this work remain open:

1. **Extended numerical search.** The current zero search was limited to $0.1 < \sigma < 1.65$ and $0 < t < 10^4$, primarily due to computational constraints. Extending the search to larger heights ($t > 10^4$) and wider real parts ($\sigma < 0.1$) would allow more reliable investigation of the asymptotic behavior of the counting function and local spacing statistics. In particular, larger datasets could provide stronger evidence for the conjectures proposed in this thesis concerning the multimodal distribution of real parts, the asymptotic growth of the counting function, and the emergence of GUE-type spacing behavior.

2. **Improved computational methods.** The current implementation relies on a computationally expensive global optimization procedure. Developing specialized algorithms for locating zeros of $P(s)$ that exploit its analytic structure (e.g., using argument principle methods or contour integration) could significantly accelerate larger-scale searches.

3. **Correlation with Riemann zeros.** Since the analytic continuation of $P(s)$ is explicitly constructed from the zeros of $\zeta(s)$, a more detailed comparison between the two zero sets would be valuable. In particular, studying cross-correlations between the imaginary parts of the zeros may help determine whether individual zeros of $P(s)$ inherit fine-scale structure from the nontrivial zeros of the Riemann zeta function.

References and sources

[1] Y. Y. Atas, E. Bogomolny, O. Giraud, G. Roux. "Distribution of the Ratio of Consecutive Level Spacings in Random Matrix Ensembles." In: *Physical Review Letters* 110.8 (2013), page 084101. https://doi.org/10.1103/PhysRevLett.110.084101.

[2] I. Belovas, R. Čepaitytė, M. Sabaliauskas. "On the zero-free region and the distribution of zeros of the prime zeta function." In: *Analele Universitatii Ovidius Constanta - Seria Matematica* 33(2) (2025), pages 27–44.

[3] I. Belovas, M. Sabaliauskas, L. Kuzma. "Series with Binomial-like Coefficients for the Investigation of Fractal Structures Associated with the Riemann Zeta Function." In: *Fractal and Fractional* 6.6 (2022). https://doi.org/10.3390/fractalfract6060300.

[4] G. Chavez, A. Allawala. "Prime zeta function statistics and Riemann zero-difference repulsion." In: *Journal of Statistical Mechanics: Theory and Experiment* 2021.7 (2021), page 073206. https://doi.org/10.1088/1742-5468/ac0ee0.

[5] H. Cohen. *High precision computation of Hardy-Littlewood constants.* URL: https://oeis.org/A221712/a221712.pdf (viewed 1998).

[6] C.-E. Fröberg. "On the prime zeta function." In: *BIT Numerical Mathematics* 8(3) (1968), pages 187–202. URL: https://doi.org/10.1007/BF01933420.

[7] J. Glaisher. "On the Sums of Inverse Powers of the Prime Numbers." In: *Quart. Jour. of Math* 25 (1891), page 347.

[8] E. Landau, A. Walfisz. "Uber die Nichfortsetzbarkeit einiger durch Dirich- letsche Reihen definierter Funktionen." In: *Rend. Circ. Math. Palermo* 44 (1920), pages 82–86.

[9] A. M. Odlyzko. "On the distribution of spacings between zeros of the zeta function." In: *Mathematics of Computation* 48.177 (1987), pages 273–308. https://doi.org/10.1090/S0025-5718-1987-0866115-0.

[10] V. Oganesyan, D. A. Huse. "Localization of interacting fermions at high temperature." In: *Physical Review B* 75.15 (2007), page 155111. https://doi.org/10.1103/PhysRevB.75.155111.

[11] F. Olver, D. Lozier, R. Boisvert, C. Clark. *NIST Handbook of Mathematical Functions.* 641 p. New York, USA: Cambridge University Press, 2010.

[12] Y. E. Tuzcu. *Prime zeta function.* 2026. URL: https://github.com/Emre905/prime_zeta_function.